DELPHI Collaboration DELPHI 2001–072 CONF 500
June 3, 2001

Search for excited leptons with the DELPHI detector at LEP

Preliminary

W. Adam[1], S. Andringa[2], M. Espírito Santo[3], P. Gonçalves[2], A. Onofre[2], L. Peralta[2], M. Pimenta[2] and B. Tomé[2]

Abstract

A search for excited leptons with the DELPHI detector at LEP is reported. The data analysed correspond to an integrated luminosity of about 539 pb^{-1} collected at centre-of-mass energies ranging from 189 GeV to 208 GeV. The search for pair-produced excited leptons establishes 95% confidence level mass limits in the region between 95 GeV/c^2 and 103 GeV/c^2, depending on the channel. The search for singly produced excited leptons establishes upper limits on the ratio of the coupling of the excited lepton to its mass (λ/m_{ℓ^*}) as a function of the mass.

Contributed Paper for EPS HEP 2001 (Budapest) and LP01 (Rome)

[1] Institut für Hochenergiephysik, Österr. Akad. d. Wissensch., Nikolsdorfergasse 18, AT-1050 Vienna, Austria
[2] LIP-IST-FCUL, Av. Elias Garcia, 14, 1, P-1000 Lisboa, Portugal
[3] CERN, CH-1211 Geneva 23, Switzerland

1 Introduction

This paper reports a search for excited leptons in DELPHI at centre-of-mass energies ($\sqrt{s}$) ranging from 189 GeV to 208 GeV.

Excited leptons (ℓ^*) are expected in models with substructure in the fermionic sector. Following the simplest phenomenological models [1], excited leptons are assumed to have both spin and isospin 1/2 and to have both their left- and right-handed components in weak isodoublets (vector-like). Form factors and anomalous magnetic moments of excited leptons are not considered in the present analysis.

The excited leptons considered in this paper couple to the photon and/or to the W/Z gauge bosons according to their internal quantum numbers and thus could be pair-produced at LEP. Single production in association with their Standard Model(SM) partners is also possible but its rate depends on the $\ell\ell^*V$ couplings, where V is a gauge boson ($V = \gamma, W, Z$) [2]. Excited lepton masses up to $\sqrt{s}$ can be probed through single production, depending on the scale Λ of the substructure, which determines the coupling.

Excited leptons are assumed to decay promptly, with decay lengths shorter than about 1 cm, as their mean lifetime for masses above 20 GeV/c^2 is predicted to be less than 10^{-15} seconds in all the cases studied.

Previous limits set by DELPHI and by other experiments can be found in references [3] and [4], respectively.

2 Production and decay of excited leptons

Pair production of charged excited leptons could proceed via s-channel γ and Z exchanges in e^+e^- collisions, while for excited neutrinos only the Z exchange contributes. Although t-channel contributions are also possible, they correspond to double de-excitation and give a negligible contribution to the overall production cross-section [1].

In the single production mode, excited leptons could result from s-channel γ and Z exchange. Important additional contributions from t-channel γ and Z exchange arise for excited electron production, while t-channel W exchange can be important for the excited electronic neutrino [1]. For the t-channel production process, the unexcited lepton is emitted preferentially at low polar angle and often goes undetected in the beam pipe.

The effective electroweak Lagrangian associated with magnetic transitions from excited leptons ℓ^* to ordinary leptons ℓ has the form

$$L_{\ell\ell^*} = \frac{1}{2\Lambda}\overline{\ell^*}\sigma^{\mu\nu}\left[gf\frac{\tau}{2}W_{\mu\nu} + g^{'}f^{'}\frac{Y}{2}B_{\mu\nu}\right]\ell_L + h.c.$$

where Λ corresponds to the compositeness mass scale, the subscript L stands for left-handed, g, $g^{'}$ are the SM gauge coupling constants and the factors f, $f^{'}$ are weight factors associated with the two gauge groups SU(2) $\times$ U(1). The meaning of these couplings and a more extensive discussion of the effective Lagrangian can be found in [1]. With the assumption $|f| = |f^{'}|$, or assuming that only one of the constants f is non-negligible, the cross-section depends simply on the parameter f/Λ, which is related to the excited lepton mass according to $f/\Lambda = \sqrt{2}\lambda/m_{\ell^*}$, where λ is the coupling of the excited lepton.

Excited leptons can decay by radiating a γ, Z or W. The decay branching ratios are functions of the f, $f^{'}$ coupling parameters of the model. Figure 1 shows the decay branching ratios of the excited leptons as a function of their mass for $f = f^{'}$ and $f = -f^{'}$.

For charged excited leptons, the electromagnetic radiative decay is forbidden if $f = -f'$, and the decay then proceeds through the Z and W bosons. However, if $f = +f'$, the electromagnetic radiative decay branching ratio is close to 100% for m_{ℓ^*} below m_W. It decreases above the W threshold, reaching a value of 34% for $m_{\ell^*} = 200$ GeV/c^2. For excited neutrinos, the situation is reversed, so that the electromagnetic partial decay width is zero if $f = +f'$. However, there is a significant contribution to the total decay width from the electromagnetic radiative decay if $f \neq f'$, even if the difference $f - f'$ is much smaller than f itself.

The process $e^+e^- \to \gamma\gamma(\gamma)$ can be used to probe compositeness at LEP and thus complement the excited electron direct searches for the mass region above the kinematic threshold. In fact, the contribution of the diagram mediated by a virtual excited electron to the $\gamma\gamma$ production cross-section would lead to a modification of the angular distribution. This effect depends on the excited electron mass m_{e^*} and on the $ee^*\gamma$ coupling, λ. The results presented in [5] will be used to extend the limits from the direct search.

Many topologies could result from the production and decay of excited leptons. The possible final states involve isolated leptons, isolated photons, jets, missing energy and missing momentum.

	Topologies	
Channel	Single production	Pair production
$\ell^* \to \ell\gamma$	$\ell\ell\gamma$, $(\ell\gamma)$	$\ell\ell\gamma\gamma$
$\ell^* \to \nu W$	$jj\ell$,(jj)	$jj\ell$,$jjjj$
$\ell^* \to \ell Z$	$jj\ell\ell$,$(jj\ell)$	-
$\nu^* \to \nu\gamma$	γ	$\gamma\gamma$
$\nu^* \to \ell W$	$jj\ell$,(jj)	$jj\ell\ell\ell$,$(jj\ell\ell)$,$jjjj\ell\ell$
$\nu^* \to \nu Z$	jj	-

Table 1: Analysed topologies corresponding to the different production and decay modes of excited leptons.

Table 1 shows the relevant topologies for the different production and decay channels. The topologies in brackets do not correspond directly to the physical final state but are often the observed ones. They become particularly important whenever there are particles produced with very low momentum or at small angle to the beam. Only the topologies that will be considered in this analysis are indicated in the table. In the single production mode the topologies arising from the leptonic decays of the W or Z and in the pair production modes the topologies corresponding to the purely leptonic decays of the WW pair are not considered due to their low branching ratio.

Single and double photon final states arise in the case of radiatively decaying excited neutrinos. For these topologies, the analyses presented in reference [5] are used.

3 Detector and data samples

A detailed description of the DELPHI detector and of its performance can be found in [6]. This analysis relies both on the charged particle detection provided by the tracking system and on the neutral cluster detection provided by the electromagnetic and hadronic calorimeters.

The luminosity collected by DELPHI from 1998 to 2000 at each centre-of-mass energy is shown in table 2. All data collected at $\sqrt{s}$ ranging from 189 GeV to 208 GeV, corresponding to a total integrated luminosity of 539 pb^{-1}, were used in the single production analysis. In the pair production search, only the data collected in the energy bins 205 GeV and 207 GeV were included up to now.

$\sqrt{s}$ (GeV)	189	192	196	200	202	205	207	208
Luminosity (pb $^{-1}$)	151.8	25.9	76.5	83.5	40.1	78.8	77.3	7.0

Table 2: Luminosity collected by DELPHI for each centre-of-mass energy. For $\sqrt{s} >$ 202 GeV the data were collected during the year 2000 and split into three energy bins.

The background process $e^+e^- \to Z\gamma$ was generated with PYTHIA 6.125 [7]. For $\mu^+\mu^-(\gamma)$ and $\tau^+\tau^-(\gamma)$, DYMU3 [8] and KORALZ 4.2 [9] were used, respectively, while the BHWIDE generator [10] was used for Bhabha events. Simulation of four-fermion final states was performed using EXCALIBUR [11] and GRC4F [12]. Compton-like final states originating from an $e\gamma$ collision (with a missing electron in the beam pipe), referred to as Compton events, were generated according to [13], and $e^+e^- \to \gamma\gamma$ events according to [14]. The two-photon ("$\gamma\gamma$") physics events were generated according to the TWOGAM [15] generator for quark channels and the Berends, Daverveldt and Kleiss generator [16] for the electron, muon and tau channels.

Single and pair excited lepton events were generated according to the cross-sections defined in [1], involving γ and Z exchange. The hadronization and decay processes were simulated by JETSET 7.4 [7]. The initial state radiation effect was included at the level of the generator for single production, while for pair production it was taken into account in the total cross-section. All the expected decay modes were included in the simulation.

The generated signal and background events were passed through the detailed simulation of the DELPHI detector and then processed with the same reconstruction and analysis programs as the real data.

4 Event selection

Many topologies could result from the production and decay of excited leptons, involving isolated leptons, isolated photons, jets and missing energy. This analysis was performed in three different steps. In the first step events with an energy greater than 20% of $\sqrt{s}$ deposited above 20° in polar angle [1] were selected and classified in topologies according

[1] The polar angle θ is defined with respect to the beam axis. In all cases also the complementary value $(180 - \theta)$ is assumed

to their multiplicity and to their number of isolated leptons and photons. In this paper, *low multiplicity* refers to events with at most five well reconstructed charged tracks.

The reconstruction of isolated particles consisted on constructing double cones centered in the direction of the charged particle tracks and of the neutral energy deposits. The energy inside an inner cone with half opening angle of 5° was required to be above 5 GeV, while the energy contained between the inner cone and the outer cone was required to be small, to ensure isolation. Both the opening angle of the outer cone and the cut on the total energy contained between the two cones were allowed to vary according to the topology of the event and to the energy and classification of the reconstructed particle. Electron, photon and muon identification were based on the standard DELPHI algorithms described in [6, 17]. Isolated photons (leptons) with an energy above 10 GeV (5 GeV) were considered.

4.1 Topologies with leptons and photons

Topologies with isolated leptons and photons are expected whenever the excited leptons (electrons, muons or taus) decay via a photon. In the single production mode, the topologies $\ell\ell\gamma$ and $\ell\gamma$ are considered. The topology with only one lepton and one photon is important for excited electron production, where the t-channel dominates, and near the kinematic limit for all flavours. Slightly different selection criteria were applied according to the flavour of the excited lepton searched for.

Events classified in $\ell\ell\gamma$ and $\ell\gamma$ topologies were selected. In the excited electron and excited muon search channels, the momentum of the most energetic lepton was required to be above 10 GeV/c. In order to reduce the background from Bhabha events in the excited electron and tau search, the isolated photon was required to be above 40° and, in the $\ell\gamma$ topology, the angle between the lepton and the photon was required to be lower than 178°.

The energies were rescaled imposing energy and momentum conservation and using the polar and azimuthal angles, which are well measured in the detector. For two-body topologies, the same method can be applied assuming the presence of a third particle along the beam direction. The compatibility of the momenta calculated from the angles with the measured momenta was quantified on a χ^2 basis [2]. Only events with $\chi^2 < 5$ either for photons or for charged particles were kept. In the $e\gamma$ topology an additional cut was applied: events with a rescaled momentum greater than $0.18\sqrt{s}$ assigned to the particle lost along the beam direction were rejected. This criterion is useful to eliminate Compton events.

In the $\ell\ell\gamma\gamma$ topology the expected background is rather low and simpler cuts were applied. Both leptons were required to have a momentum above 10 GeV/c. In the signal, the mass of the decaying lepton should be given by the lepton-photon invariant masses in the event, once the good pairing is found. Events were kept as candidates if a pairing could be found for which the difference between the two lepton-photon invariant masses was lower than 15 GeV/c^2 in the excited electron or muon channels and 20 GeV/c^2 in the

[2]The χ^2 parameter was defined separately for charged jets ($\chi^2_{charged}$) and photons ($\chi^2_{photons}$) as $\chi^2 = \frac{1}{n}\sum_{i=1,n}\left(\frac{p_i^{calc}-p_i^{meas}}{\sigma_i}\right)^2$ where n is the number of measured particles, p_i^{meas} are the measured momenta or energies and p_i^{calc} are the momenta calculated from the kinematic constraints. σ_i, the quadratic sum of the errors on p_i^{calc} and p_i^{meas}, is defined in reference [3]

tau channel.

In all cases, events were kept as candidates in the excited electron channel if both leptons were identified as electrons, and in the excited muon channel if the most energetic lepton was identified as a muon and the other was not identified as an electron. In the excited tau channel, a difference between the measured and rescaled momenta of the leptons characteristic of the presence of neutrinos from tau decays was required, imposing $\chi^2_{charged} > 5$ ($\chi^2_{charged} > 10$ in the $\ell\ell\gamma\gamma$ topology).

Figure 2 shows distributions for the $\ell\ell\gamma$ topology at the first level of the event selection for $\sqrt{s}$ =207 GeV. There is a reasonable agreement between the data and SM simulation.

4.2 Topologies with jets and leptons

4.2.1 Single production analysis

In high multiplicity events from single excited lepton production the jets originate from the decay of a W or a Z which is not produced at rest. The candidates were required to have two charged jets with high acollinearity (A^{jj}_{col}), acoplanarity (A^{jj}_{cop}) [3] and mass M_{jj}. The relevant topologies are jj, $jj\ell$ and $jj\ell\ell$. The main backgrounds for these topologies are $e^+e^- \to q\overline{q}(\gamma)$ events, including radiative returns to the Z ($e^+e^- \to Z\gamma$) where the photon is lost in the beam pipe, and semileptonic decays of W pairs. In the first case the events are characterized by two acollinear jets. Radiative return events have a high missing momentum ($\not{p}$) at low polar angle ($\theta(\overrightarrow{\not{p}})$). In semileptonic WW events the mass recoiling against the 2-jet system (M_R) is close to the W mass.

High multiplicity events were clustered into jets using the Durham algorithm [18]. Two jet events were selected by requiring the Durham resolution variable in the transition from three to two jets (two to one jet) to be lower than 0.06 (greater than 0.01).

In the jj topology, events were kept if $A^{jj}_{col} > 60°$, $A^{jj}_{cop} > 25°$, $50 < M_{jj} < 100$ GeV/c^2, $\theta(\overrightarrow{\not{p}}) > 25°$ and the polar angle of the most energetic jet (θ_j) was greater than 20°. Fully hadronic WW event rejection was achieved by cutting tighter in the Durham resolution variable: $y_{cut(3\to2)} < 0.01$.

Similar but looser cuts were applied in the case of the $jj\ell$ topology. Events were kept if $A^{jj}_{col} > 30°$, $A^{jj}_{cop} > 15°$, $M_{jj} > 40$ GeV/c^2, $\theta(\overrightarrow{\not{p}}) > 20°$ and $\theta_j > 20°$.

If two isolated leptons were found in the event looser cuts were applied: $A^{jj}_{col} > 20°$, $A^{jj}_{cop} > 10°$ and $\theta(\overrightarrow{\not{p}}) > 20°$. The isolation angle of the least energetic lepton had to be greater than 20°.

In order to improve the estimation of the momentum and energy of the jets a kinematic constrained fit was applied to the selected events. The constraints imposed depended on the particular final state being studied. In several of the relevant final states, jet pairs come from the decay of W or Z bosons. Therefore, the invariant mass of the two-jet system can be required to be either m_W or m_Z. Since the jj and $jj\ell$ topologies can arise from both the W and the Z channels the fit was performed twice for these topologies, using m_W and m_Z. For the $jj\ell\ell$ topology the fit was performed requiring the invariant mass of the two-jet system to be m_Z. The details of the fitting procedure, including the errors on the input variables, can be found in reference [19]. After the fit only events with a χ^2 per degree of freedom lower than 5 were retained.

[3] The acoplanarity is defined in the plane perpendicular to the beam.

In the last step of the analysis, the different production and decay modes within the same topology were treated separately: the flavour information of the final state leptons was used, and the mass recoiling against the two jet system was required to be below 60 GeV/c^2 and 75 GeV/c^2 in the search for decays via a W or a Z boson, respectively.

Data and SM simulation distributions at $\sqrt{s}$ =207 GeV for the high multiplicity topologies at preselection level are shown in figure 3.

4.2.2 $\nu^*\nu^*$ search

For the search of pair produced neutral excited leptons ($\nu^*\nu^* \to \ell W \ell W$) only the *fully hadronic* and *semileptonic* cases (referring to the decay mode of the pair of W bosons in the final state) were taken into account. In the final state we have, thus, besides the W decay products (two jets and one lepton or four jets), two additional charged leptons which constitute a rather clear signature.

Multijet events were selected requiring $y_{cut(2\to1)} > 0.03$. Events with at least two isolated leptons were kept. If exactly two isolated leptons were found, background from ZZ events was rejected by requiring that $y_{cut(3\to2)} > 0.01$.

In the search for excited neutrinos of first and second family the charged leptons in the final state were required to be of the corresponding flavour. In the search of third family excited neutrinos, a missing energy greater than $0.1\sqrt{s}$ was demanded.

4.2.3 $\ell^*\ell^*$ search

In the charged excited leptons search channels, contrary to the neutral case described in the previous section, the two additional leptons in the final state are neutrinos, seen as missing energy, and the background from WW events is nearly irreducible. For this reason, a discriminant analysis was used in this channel. After the event preselection a signal likelihood $\mathcal{L}_S$ and a background likelihood $\mathcal{L}_B$ were constructed as the product of probability density functions (PDFs) of relevant kinematic variables. The discriminating variable was defined as $\mathcal{L}_S/\mathcal{L}_B$.

The relevant topologies for the pair production of charged excited leptons are two jets and one lepton or four jets, resulting from the decay of the two W bosons. The *fully hadronic* and *semileptonic* cases were treated separately.

In the *semileptonic* analysis events with no isolated photons and at least one isolated lepton were considered and the remaining particles were clustered into jets. Two jet events were selected by cutting in the Durham resolution variables as in section 4.2.1. QCD background was reduced by requiring the polar angle of the direction of the missing momentum to be above 20°. The lepton energy and its minimum transverse momentum with respect to the jets had to be greater than 10 GeV; the lepton polar angle was required to be above 20° (40°) for muons (electrons). The following variables were then used to build the discriminant variable:

- missing energy of the event,
- angle between the two jets,
- energy of the lepton,
- angle between the lepton and the direction of the missing momentum,

- the product of the lepton momentum and its charge.

In the *fully hadronic* analysis it was required that no isolated photons or leptons were present. Four jet event were selected requiring $y_{cut(4\to3)} > 0.003$ and $y_{cut(3\to2)} > 0.03$ A fit imposing energy-momentum conservation and the W mass for two jet pairs was performed. The following quantities were then used to build the discriminant variable:

- missing energy of the event,
- angle between the two jets in each of the two pairs,
- angle between the two reconstructed $W's$.

The distributions of relevant variables in data and background simulation at the preselection level are shown in figure 4. A good agreement is observed.

The discriminant variable is shown, for both the *hadronic* and the *semileptonic* case, in figure 5.

5 Results

For a given excited lepton production and decay mode several final state topologies might contribute. The relevance of each topology depends on the decay branching ratios which are a function of the excited lepton mass and of the coupling parameters.

The numbers of excited lepton candidates in the single production topologies, as well as the SM expectations, are summarized in tables 3 to 5 for the different excited lepton types and decay modes and for the different centre-of-mass energies. It should be noted that these numbers result from the combination of the different topologies and there is, in many cases, overlap between the candidates selected in the different search channels.

The signal efficiencies are given in table 6 for all the studied channels and for specific excited lepton mass values at $\sqrt{s} = 206$ GeV. The efficiencies are very similar for equivalent masses (in terms of distance to the kinematic limit) at the other centre-of-mass energies. The dependence of the efficiency on the mass is weak, due to the combination of the several topologies and of the different centre-of-mass energies.

In many topologies, the excited lepton mass can be estimated from the momenta and directions of final state particles. Relevant cases are the $\ell\gamma$ invariant mass for radiatively decaying excited leptons, the jet-jet-lepton invariant mass and the recoil mass of isolated leptons for the situations involving W and Z bosons. The mass resolution on the lepton-photon invariant mass, after applying the kinematic constraints, was found to be about 1 GeV/c^2 for muons, 1.5 GeV/c^2 for electrons and 2 GeV/c^2 for taus. In high multiplicity events with isolated leptons, the resolution on the lepton recoil mass is about 1 GeV/c^2 for muons, 3 GeV/c^2 for electrons and 5 GeV/c^2 for taus. The resolution on the jet-jet-lepton invariant mass is about 5 GeV/c^2 for muons and 8 GeV/c^2 for electrons; no mass reconstruction was attempted in the tau channel. Events for which the mass could not be estimated were treated as candidates for all possible mass values.

6 Limits

Limits were computed using the likelihood ratio method described in [20]. This method is well suited both for the combination of channels and for the inclusion of mass information.

Each topology at each centre-of-mass energy was treated as a channel, and the mass resolution used depended on the specific reconstruction procedure for each topology.

For the single production of excited leptons, the production cross-section is a function not only of the mass of the particle but also of the ratio of the coupling of the excited lepton to its mass. 95% confidence level (CL) upper limits on the ratio λ/m_{ℓ^*} as a function of the ℓ^* mass were derived. Figures 6 and 7 show these limits for the excited leptons assuming $f = f'$ and $f = -f'$ respectively.

Lower limits at 95% CL on the masses of pair-produced excited leptons are given in table 7. Limits are given for $f = f'$ and $f = -f'$.

Figure 8 shows the limit on the excited electron production for $f = f'$ obtained by combining the result of the direct search (figure 6(a)) with the indirect result from the search for deviations in the $e^+e^- \to \gamma\gamma(\gamma)$ differential cross-section [5]. We can thus extend the exclusion to regions above the kinematic limit.

7 Conclusions

DELPHI data corresponding to integrated luminosities of 539 pb^{-1}, at centre-of-mass energies ranging from 189 GeV to 208 GeV have been analysed. A search for excited leptons decaying promptly through γ, Z or W emission was performed. No significant signal was observed.

The search for pair production of excited leptons resulted in the mass limits quoted in table 7. The search for single production of excited leptons gave the limits on the ratio λ/m^*_ℓ shown in Figures 6, 7 and 8. These results considerably extend the limits set by LEP and HERA [3, 4].

Acknowledgements

We are greatly indebted to our technical collaborators and to the funding agencies for their support in building and operating the DELPHI detector. Very special thanks are due to the members of the CERN-SL Division for the excellent performance of the LEP collider.

References

[1] K. Hagiwara, S. Komamiya and D. Zeppenfeld, Z. Phys. **C29** (1985) 115;
F. Boudjema, A. Djouadi and J.L. Kneur, Z. Phys. **C57** (1993) 425.

[2] A. Djouadi, Zeit. Phys. **C63** (1994) 317.

[3] DELPHI Coll., P. Abreu et al., E. Phys. J. **C8** (1999) 41; DELPHI Coll., P. Abreu et al., Phys. Lett. **B380** (1996) 480.

[4] ALEPH Coll., T. Medcalf et al., "Search for excited leptons in e+e- collisions at sqrts = 188.6 GeV", CERN-OPEN 99-171, contributed paper to EPS-HEP99;
L3 Coll., M. Acciarri et al., "Search for Excited Leptons in e^+e^- Interactions at $\sqrt{s}$=192-202 GeV", CERN-EP-2000-143 (2000), submitted to Phys. Lett. B;

OPAL Coll., G. Abbiendi et al., E. Phys. J. **C14** (2000) 73;
H1 Coll., C. Adloff et al., Eur. Phys. J. **C17** (2000) 567;
ZEUS Coll., J. Breitweg et al.,Z. Phys. **C76** (1997) 631.

[5] S. Andringa et al.,"Determination of the $e^+e^- \to \gamma\gamma(\gamma)$ cross-section using data collected with the DELPHI detector up to the year 2000", contribution to Rencontres de Moriond (march 2001);
DELPHI Coll., P. Abreu et al., Phys. Lett. **B491** (2000) 67;
DELPHI Coll., P. Abreu et al., Eur. Phys. J. **C17**(2000) 187.

[6] DELPHI Coll., P. Aarnio et al., Nucl. Instr. Methods **A303** (1991) 233;
DELPHI Coll., P. Abreu et al., Nucl. Instr. Methods **A378** (1996) 57.

[7] T. Sjöstrand, Comp. Phys. Comm. **82** (1994) 74;
T. Sjöstrand, Pythia 5.7 and Jetset 7.4, CERN-TH/7112-93.

[8] J.E. Campagne and R. Zitoun, Z. Phys. **C43** (1989) 469.

[9] S. Jadach, B.F.L. Ward and Z. Wąs, Comp. Phys. Comm **66** (1991) 276.

[10] S. Jadach, W. Placzek and B.F.L. Ward, Phys. Lett. **B390** (1997) 298.

[11] F.A. Berends, R. Pittau and R. Kleiss, Comp. Phys. Comm **85** (1995) 437.

[12] J.Fujimoto et al., Comp. Phys. Comm. **100** (1997) 128.

[13] D. Karlen, Nucl. Phys. **B289** (1987) 23.

[14] F. Berends and R. Kleiss, Nucl. Phys. **B186** (1981) 22.

[15] S. Nova, A. Olchevski and T. Todorov, "TWOGAM, CERN report 96-01, vol.2 p. 224 (1996).

[16] F.A. Berends, P.H. Daverveldt and R. Kleiss, Comp. Phys. Comm. **40** (1986) 271.

[17] F.Cossutti et al., "REMCLU : a package for the Reconstruction of Electromagnetic CLUsters at LEP200", DELPHI Note 2000-164 PROG 242.

[18] S. Catani et al., Phys. Lett. **B269** (1991) 432.

[19] DELPHI Coll., P. Abreu et al., Eur. Phys. J. **C2** (1998) 581.

[20] A.L. Read, "Optimal statistical analysis of search results based on the likelihood ratio and its application to the search for the MSM Higgs boson at $\sqrt{s}$=161 and 172 GeV", DELPHI note 97-158 PHYS 737.

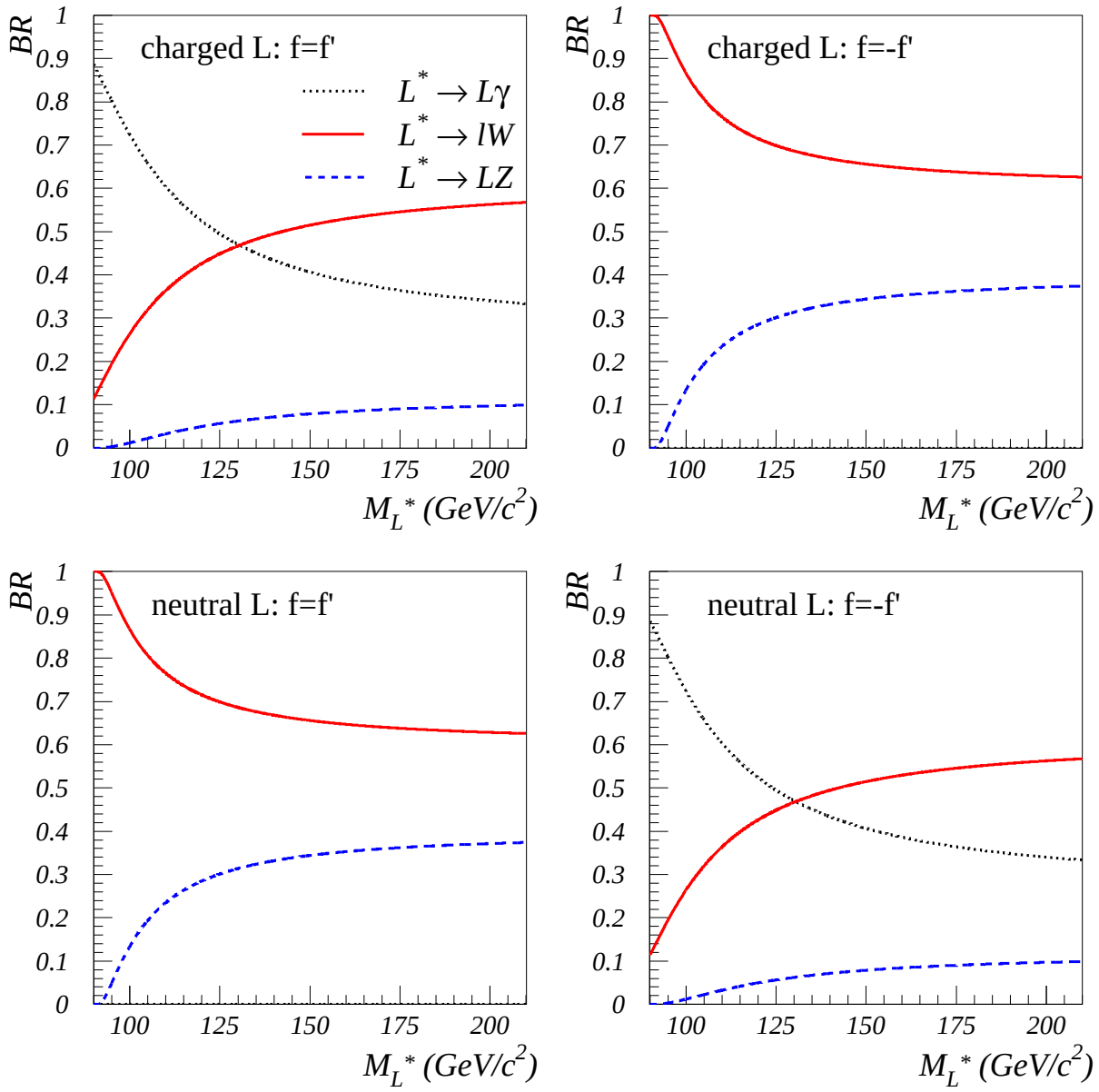

Figure 1: Branching-ratios for excited lepton decays as a function of the mass for $f = +f^{'}$ and $f = -f^{'}$ (upper part for excited charged leptons and lower part for excited neutrinos).

$\sqrt{s}$ GeV	topology	lepton id.		
		e	μ	τ
189	$\ell^* \to \ell\gamma$	144(128±6)	28(37±2)	62(49±4)
	$\ell^* \to \nu W$	38(42±3)	22(21±2)	12(14±1)
	$\ell^* \to \ell Z$	87(96±4)	52(51±3)	86(81±4)
	$\nu^* \to \nu\gamma$	3(0.7)		
	$\nu^* \to \ell W$	34(38±3)	18(17±2)	33(30±3)
	$\nu^* \to \nu Z$	13(9±1)		
192	$\ell^* \to \ell\gamma$	22 (20±1)	11 (8.4±0.4)	19 (13±1)
	$\ell^* \to \nu W$	6 (5.8±0.6)	2 (3.2±0.3)	1(1.5±0.2)
	$\ell^* \to \ell Z$	11 (13.5±0.7)	6 (9.6±0.5)	6 (7.6±0.5)
	$\nu^* \to \nu\gamma$	0 (0.1)		
	$\nu^* \to \ell W$	6 (5.2±0.6)	2 (2.6±0.3)	4 (2.8±0.3)
	$\nu^* \to \nu Z$	0(1.2±0.1)		
196	$\ell^* \to \ell\gamma$	51 (59±4)	22 (24±1)	50 (38±3)
	$\ell^* \to \nu W$	14 (17±2)	11 (9.7±0.8)	5 (4.6±0.7)
	$\ell^* \to \ell Z$	44 (41±2)	22 (29±1)	28(23±2)
	$\nu^* \to \nu\gamma$	2 (0.7)		
	$\nu^* \to \ell W$	12 (15±2)	9 (7.9±0.8)	8 (9±1)
	$\nu^* \to \nu Z$	1 (3.7±0.4)		
200	$\ell^* \to \ell\gamma$	62 (63±4)	27 (26±1)	45 (42±3)
	$\ell^* \to \nu W$	21 (22±2)	13 (13±1)	11 (7±1)
	$\ell^* \to \ell Z$	46 (52±3)	33 (31±1)	28 (24±2)
	$\nu^* \to \nu\gamma$	6 (1.7)		
	$\nu^* \to \ell W$	18 (20±2)	10 (11±1)	15 (14±1)
	$\nu^* \to \nu Z$	4 (4.3±0.5)		

Table 3: Number of candidates for the different excited lepton decay channels in the single production modes, at $\sqrt{s}$ in the range 189 to 200 GeV. The numbers in brackets correspond to the SM background expectations, with their statistical errors.

$\sqrt{s}$		lepton id.		
GeV	topology	e	μ	τ
202	$\ell^* \to \ell\gamma$	39 (30±2)	10 (12.5±0.5)	26 (20±2)
	$\ell^* \to \nu W$	10 (11±1)	5(6.5±0.5)	1 (3.5±0.5)
	$\ell^* \to \ell Z$	27 (25±1)	13(15.1±0.7)	13 (11.8±0.9)
	$\nu^* \to \nu\gamma$	1 (1.2)		
	$\nu^* \to \ell W$	9 (10±1)	4 (5.4±0.5)	6 (6.6±0.7)
	$\nu^* \to \nu Z$	1 (2.1±0.2)		
205	$\ell^* \to \ell\gamma$	71 (63±3)	20 (21±1)	29 (22±2)
	$\ell^* \to \nu W$	9 (13±1)	12 (12.5±0.7)	3 (6.2±0.6)
	$\ell^* \to \ell Z$	28 (30±1)	28 (32±1)	32 (24±1)
	$\nu^* \to \nu\gamma$	5 (1.3)		
	$\nu^* \to \ell W$	7 (10.0±0.8)	10 (10.0±0.7)	7 (10.4±0.8)
	$\nu^* \to \nu Z$	7 (5.0±0.4)		
207	$\ell^* \to \ell\gamma$	65 (60±3)	21 (21.8±0.8)	22 (21±2)
	$\ell^* \to \nu W$	11 (13.0±0.8)	13 (12.0±0.6)	7 (6.0±0.5)
	$\ell^* \to \ell Z$	35 (32±1)	26 (31±1)	24 (28±1)
	$\nu^* \to \nu\gamma$	1 (2.6)		
	$\nu^* \to \ell W$	7 (10.9±0.8)	9 (9.8±0.6)	11 (10.0±0.8)
	$\nu^* \to \nu Z$	7 (5.2±0.5)		
208	$\ell^* \to \ell\gamma$	5 (4.3±0.3)	2 (1.62±0.06)	1 (1.5±0.1)
	$\ell^* \to \nu W$	1 (1.18±0.08)	3 (1.17±0.06)	0 (0.57±0.05)
	$\ell^* \to \ell Z$	1 (3.0±0.1)	4 (2.9±0.1)	2 (2.5±0.1)
	$\nu^* \to \nu\gamma$	- (-)		
	$\nu^* \to \ell W$	1 (0.97±0.07)	3 (0.96±0.06)	0 (0.93±0.07)
	$\nu^* \to \nu Z$	0 (0.50±0.04)		

Table 4: Number of candidates for the different excited lepton decay channels in the single production modes, at $\sqrt{s}$ in the range 202 to 208 GeV. and centre-of-mass energies. The numbers in brackets correspond to the SM background expectations with their statistical errors.

$\sqrt{s}$	channel	e	μ	τ
205 GeV	$\ell^* \to \ell\gamma$	0(1.9±0.3)	0(0.5±0.1)	2(3.4±0.4)
	$\nu^* \to \nu\gamma$	2(2.5±0.3)		
	$\ell^* \to \nu W$ (hadr.)	415(428±6)		
	$\ell^* \to \nu W$ (semilep.)	256(235±3)		
	$\nu^* \to \ell W$	2(3.9±0.4)	2(1.3±0.1)	19(17.1±0.9)
207 GeV	$\ell^* \to \ell\gamma$	2(1.8±0.3)	1(0.5±0.1)	4(3.3±0.4)
	$\nu^* \to \nu\gamma$	0(2.6±0.3)		
	$\ell^* \to \nu W$ (hadr.)	411(420±5)		
	$\ell^* \to \nu W$ (semilep.)	218(238±3)		
	$\nu^* \to \ell W$	4(3.5±0.3)	2(1.3±0.1)	16(15.9±0.7)
208 GeV	$\ell^* \to \ell\gamma$	0(0.16±0.03)	0(0.04±0.01)	0(0.29±0.03)
	$\nu^* \to \ell W$	0(0.30±0.03)	0(0.11±0.02)	2(1.52±0.08)

Table 5: Number of excited lepton candidates for the different decay channels and the different centre-of-mass energies in the pair production modes, at $\sqrt{s}$ in the range 205 GeV to 208 GeV. The numbers in brackets correspond to the SM background expectations with their statistical errors.

channel	lepton id.		
	e	μ	τ
$\ell^* \to \ell\gamma$	26	60	23
$\ell^* \to \nu W$	20	30	20
$\ell^* \to \ell Z$	18	39	20
$\nu^* \to \nu\gamma$	35		
$\nu^* \to \ell W$	30	35	15
$\nu^* \to \nu Z$	18		

channel	e	μ	τ
$\ell^* \to \ell\gamma$	39	52	18
$\ell^* \to \nu W$ (hadr.)	22		
$\ell^* \to \nu W$ (semilep.)	17		
$\nu^* \to \nu\gamma$	50		
$\nu^* \to \ell W$	28	42	13

Table 6: Selection efficiency (in %) for the different excited lepton flavours and decay channels, in the single (left table) and pair (right table) production modes for m_{ℓ^*}=200 GeV (single) and m_{ℓ^*}=100 GeV (pair) at $\sqrt{s}$ =206 GeV. The statistical errors are of the order of 2%.

	e^*	μ^*	τ^*
$f = f'$	103.0	103.1	102.2
$f = -f'$	98	98	98

	ν_e^*	ν_μ^*	ν_τ^*
$f = f'$	102.0	102.4	95.3
$f = -f'$	102.7	102.8	102.8

Table 7: Lower limits (in GeV/c^2) at 95 % CL on the excited lepton masses from the pair production modes.

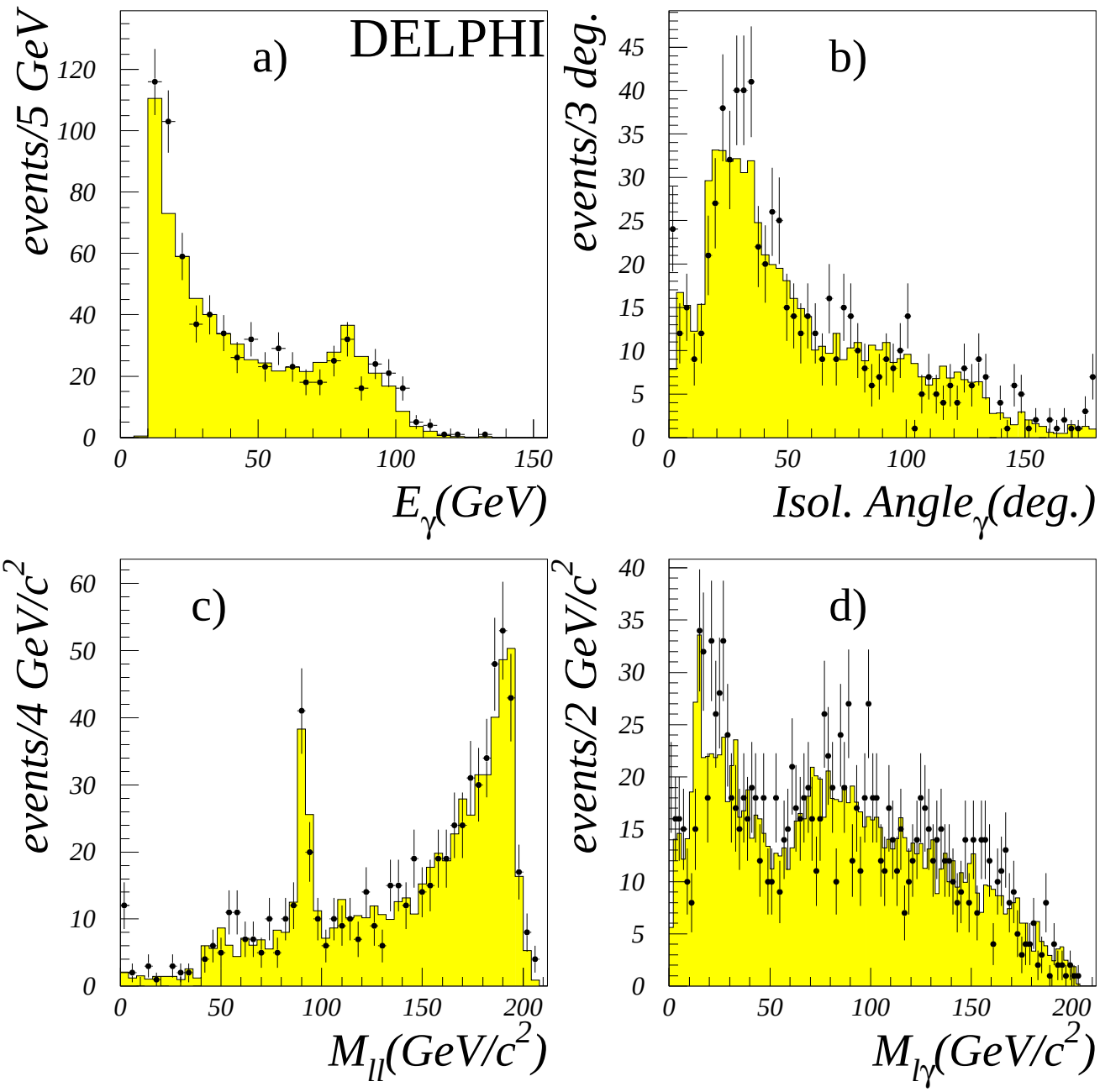

Figure 2: Energy **(a)** and isolation angle **(b)** of the photon, invariant mass of the two leptons **(c)**, invariant mass of lepton-photon pairs **(d)**, for the $\ell\ell\gamma$ topology at 207 GeV. The dots show the data and the shaded histograms show the SM simulation.

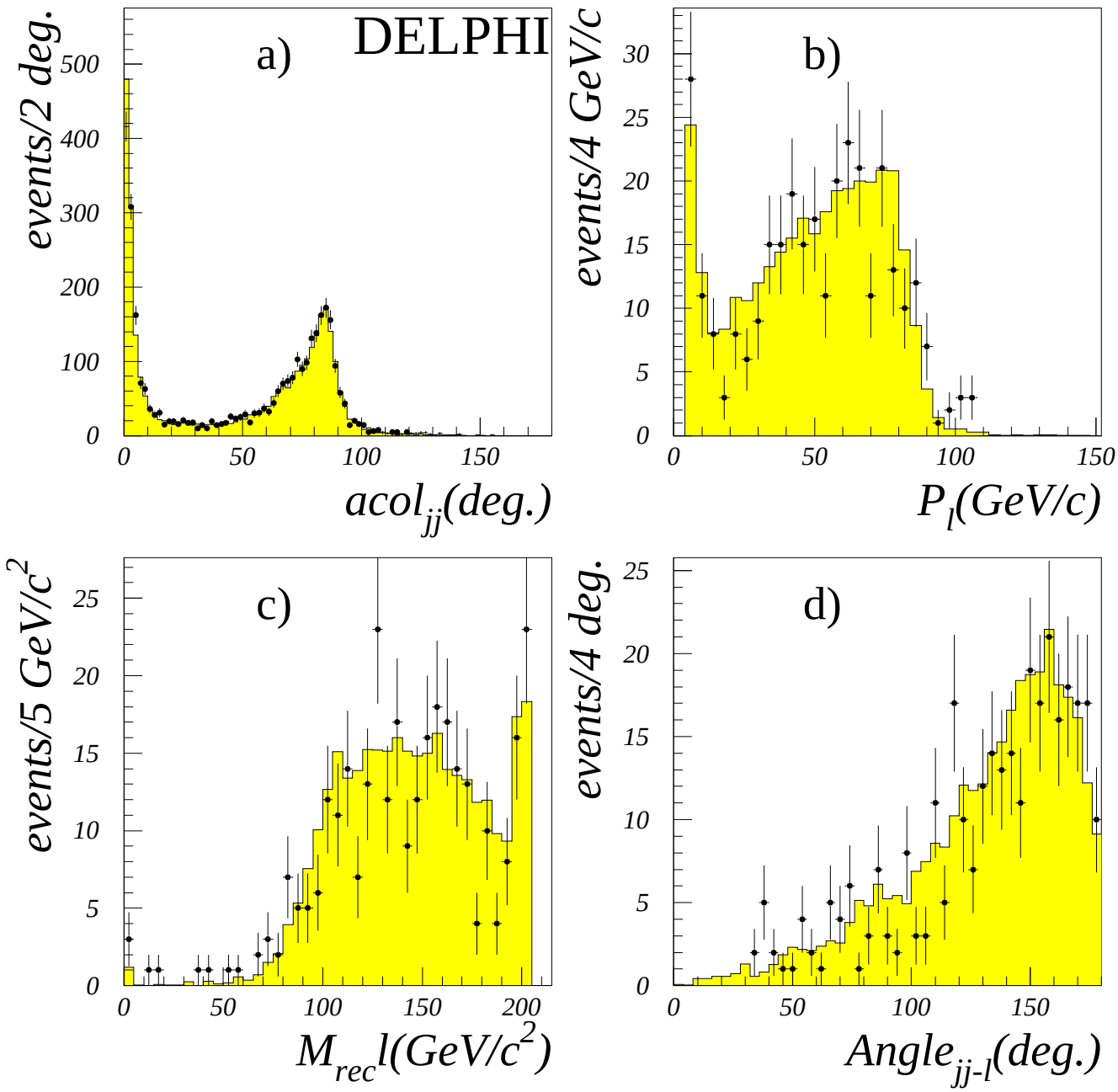

Figure 3: Acolinearity of the 2 jets in the jj topology **(a)**; $jj\ell$ topology: momentum of the lepton **(b)**, mass recoiling against the lepton **(c)**, angle between the jet pair and the lepton **(d)**, at $\sqrt{s}$ =207 GeV. The dots show the data and the shaded histograms show the SM simulation.

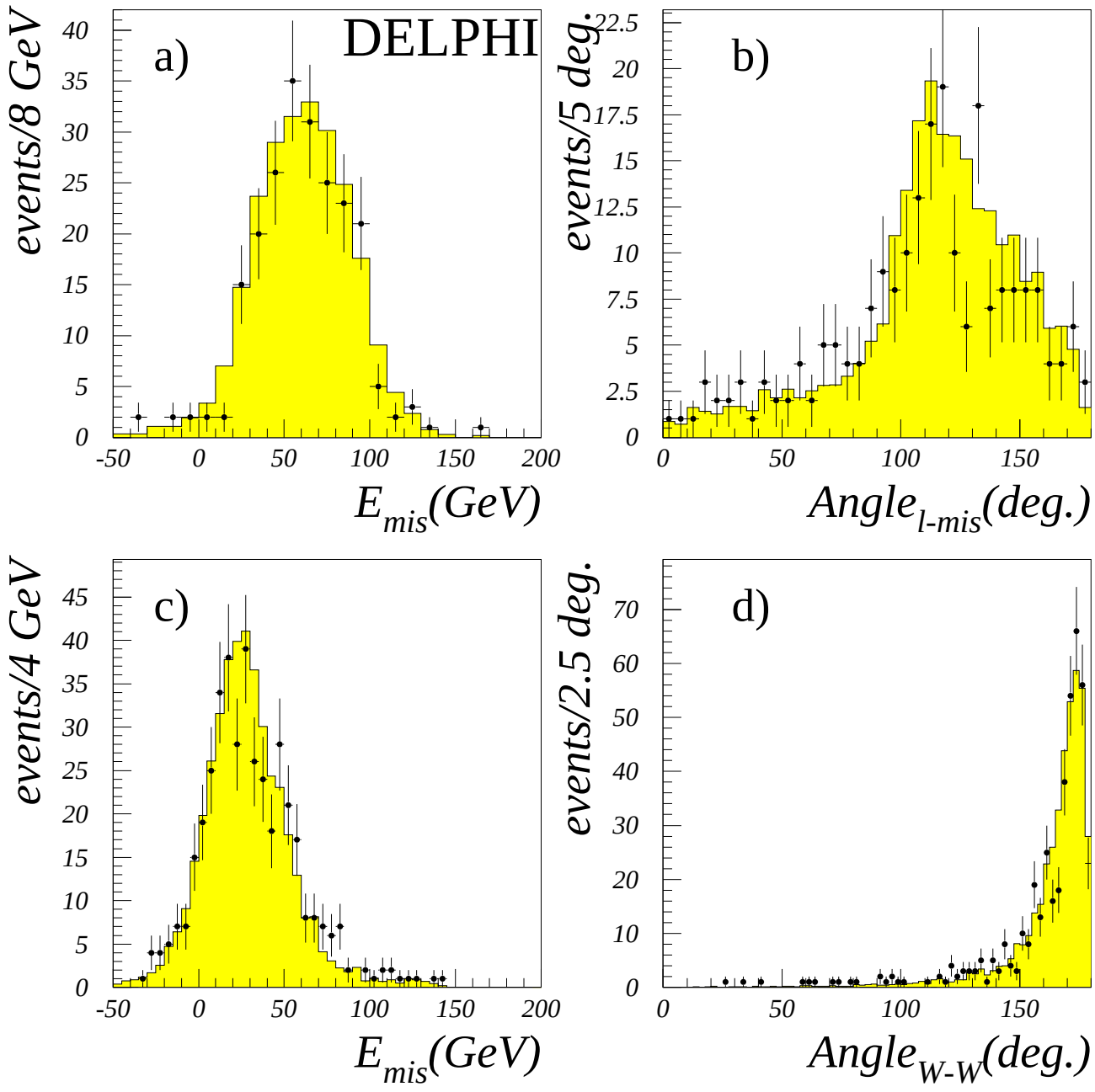

Figure 4: $\ell^*\ell^*$ search: missing energy **(a)** and angle between the lepton and the direction of the missing momentum **(b)** in the *semileptonic* channel; missing energy **(c)** and angle between the two reconstructed Ws **(d)** in the *fully hadronic* channel, at $\sqrt{s}$ =207 GeV. The dots show the data and the shaded histograms show the SM simulation.

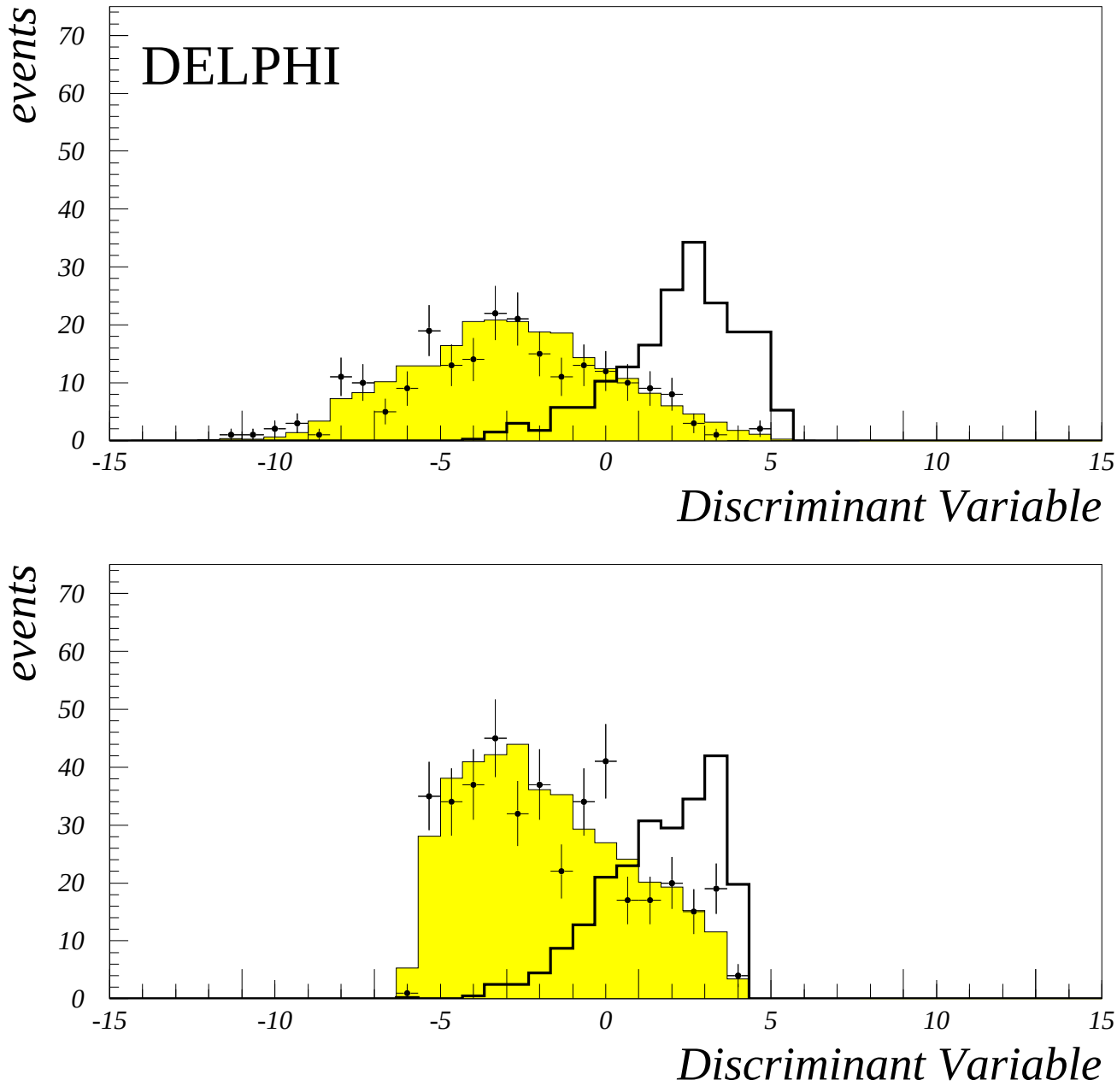

Figure 5: $\ell^*\ell^*$ search: discriminat variables in the *semileptonic* (upper plot) and *fully hadronic* (lower plot) channels at $\sqrt{s}$ =207 GeV. The dots are the data and the shaded histogram is the SM background expectation. The thick line shows a signal with m^*_ℓ=95 GeV/c^2.

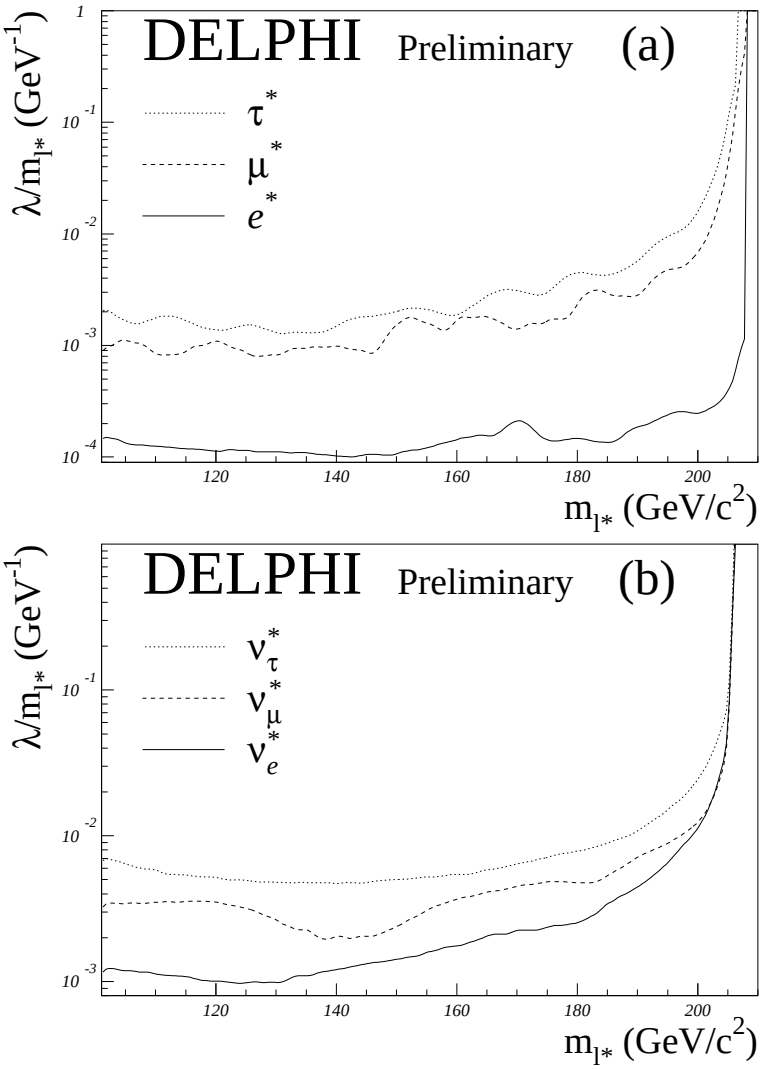

Figure 6: Results on single production of excited charged (upper plot) and neutral (lower plot) leptons assuming $f = +f'$. The lines show the upper limits at 95% CL on the ratio λ/m_{ℓ^*} between the coupling of the excited lepton and its mass as a function the mass.

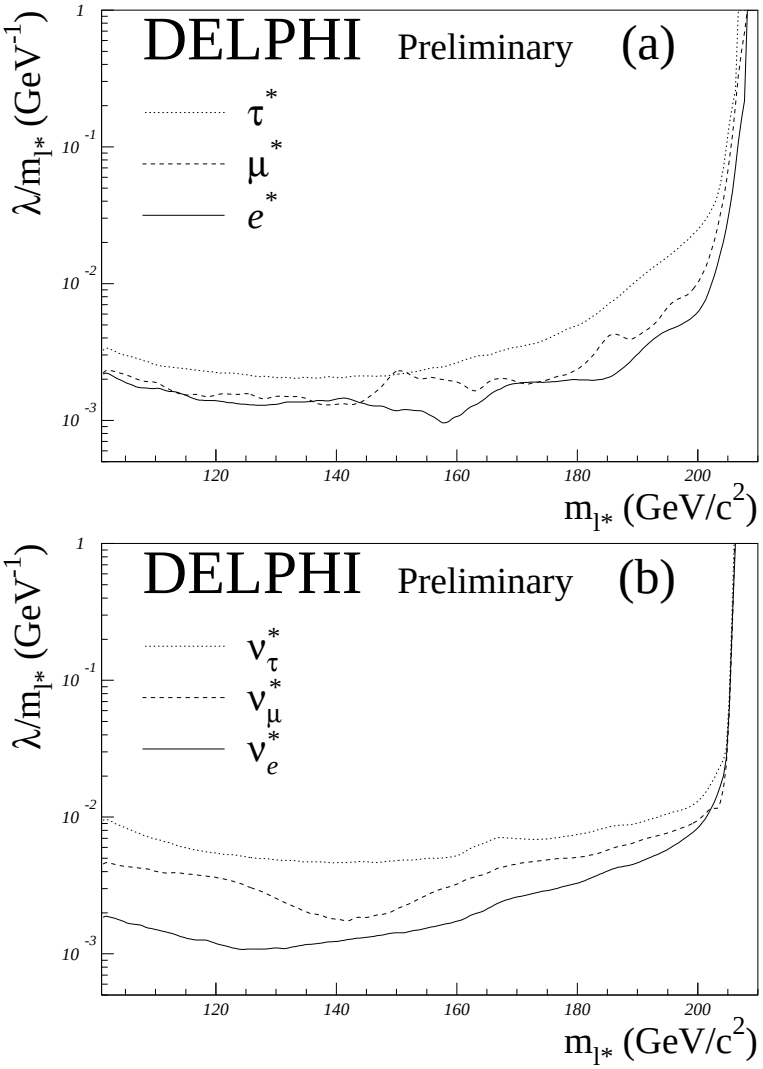

Figure 7: As figure 6, but for $f = -f'$.

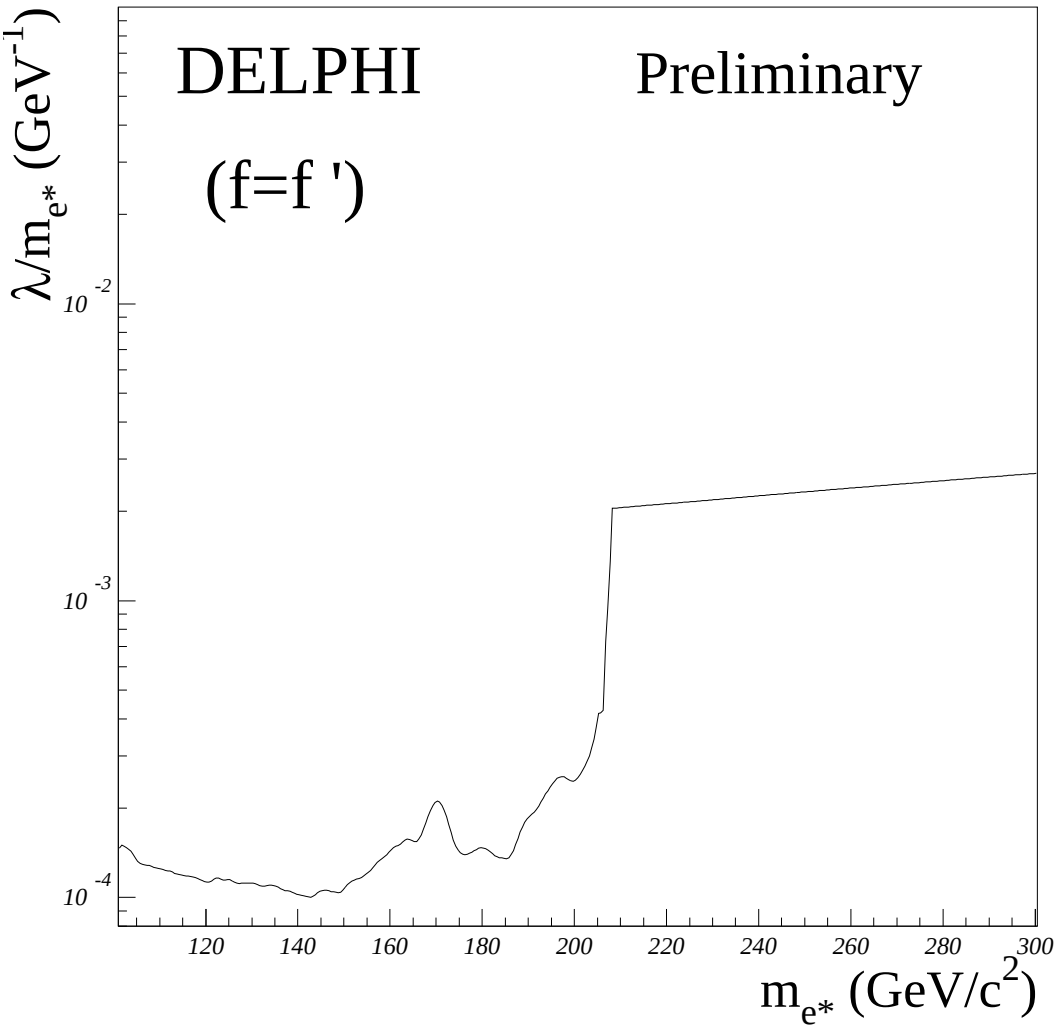

Figure 8: Combined limit on excited electron production for $f = f'$ from direct and indirect searches. The line shows the upper limit at 95% CL on the ratio λ/m_{e^*}. Up to the kinematic limit the result is dominated by the single production direct search. Above this value, the limit is the one resulting from the indirect search using $e^+e^- \to \gamma\gamma$.